Hindawi
International Journal of Photoenergy
Volume 2021, Article ID 6651541, 8 pages
https://doi.org/10.1155/2021/6651541

Research Article

The Effect of Graphite and Fe_2O_3 Addition on Hydrolysis Kinetics of Mg-Based Hydrogen Storage Materials

Kun Yang,[1] **Hongyun Qin**,[1] **Junnan Lv**,[1] **Rujun Yu**,[1] **Xia Chen**,[1] **Zengdian Zhao**,[1] **Yongjie Li**,[1] **Fang Zhang**,[2] **Xianchang Xia**,[2] **Qiang Fu**,[1] **and Ming Wang**[1]

[1]*School of Chemistry and Chemical Engineering, Shandong University of Technology, Zibo 255049, China*
[2]*Consultant Beijing, 10080, China*

Correspondence should be addressed to Qiang Fu; fuqiang@tju.edu.cn and Ming Wang; wangming@zhongxunhb.com

Received 20 November 2020; Revised 28 December 2020; Accepted 5 February 2021; Published 24 February 2021

Academic Editor: Umapada Pal

In this paper, graphite and Fe_2O_3 are introduced into MgH_2 powder by the method of hydrogenation after magnetic grinding. Hydrogen storage materials which composite of MgH_2–5 wt.% C and MgH_2–5 wt.% C–5 wt.% Fe_2O_3 are successfully prepared. The physical structure of these materials was analyzed and characterized by XRD, SEM, etc. Furthermore, the influence of graphite and Fe_2O_3 on the hydrolysis of MgH_2 was systematically investigated. The results show that MgH_2–C–Fe_2O_3 composite powder has the fastest hydrogen release rate in municipal drinking water and the highest conversion rate. Graphite and Fe_2O_3 can effectively reduce the activation energy of the hydrolysis reaction of MgH_2 and improve the hydrolysis kinetics of MgH_2. The synergistic effect of the coaddition of graphite and Fe_2O_3 can significantly increase the hydrolysis conversion rate of MgH_2 and improve the hydrolysis kinetics.

1. Introduction

Due to the increasing environmental pollution caused by the development and use of fossil fuels such as petroleum, the research and use of green and clean energy has become an increasing focus of the society [1–3]. Hydrogen is an ideal clean energy, whose energy density ($142\,MJ\,kg^{-1}$) is three times that of gasoline, and the combustion product is only water [4]. In the past few decades, most of the commercial hydrogen was obtained through partial oxidation of natural gas and coal gasification [5], which consumes petrochemical energy to cause certain environmental pollution. Recently, hydrogen production by hydrolysis has become a new focus due to its simple process, mild reaction conditions, safety, clean, and efficiency [6–8]. Researchers have reported several materials for hydrogen production by hydrolysis, such as metals [9], metal hydrides [10, 11], and borohydrides [12–14]. Among all the hydrogen storage materials, MgH_2 has the advantages of large hydrogen storage capacity (7.6 wt.%) and high theoretical hydrolysis hydrogen production (15.2 wt.%). In recent years, it has attracted much attention from scientific researchers. Hydrogen can be obtained by the reaction of MgH_2 with water, and the reaction equation is as follows:

$$MgH_2 + 2H_2O \rightarrow Mg(OH)_2 + 2H_2\uparrow \Delta H = -277\,kJmol^{-1}. \quad (1)$$

The hydrolysis reaction of MgH_2 is not harsh and can proceed spontaneously in contact with water at room temperature. However, a passivation layer can be formed on the surface of the unreacted MgH_2 during the hydrolysis process, which prevents the water from diffusing into the interior, thus, making the hydrolysis stop rapidly from the high-speed reaction stage. Kojima et al. [15] reported that the hydrogen conversion rate of MgH_2 hydrolysis is less than 30% in municipal drinking water for 1 hour, which hinders the practical application of MgH_2. For improving the low conversion rate of MgH_2 hydrolysis, many studies have been reported, such as reducing the particle size of MgH_2 to nanometer [16, 17] and using other aqueous solutions (such as

acid solution [18] and salt solution [19–21]) to prevent the generation of $Mg(OH)_2$ passivation layer. In addition, adding chloride [22], metal hydride [23, 24], carbon material [25, 26], and metal oxide [27, 28] to MgH_2 by ball grinding and other methods can also significantly improve the hydrolysis kinetic performance of MgH_2. For example, Yang et al. [28] studied the effects of TiO_2, $MgAl_2O_4$, and Fe on the hydrolysis properties of MgH_2. As an amphoteric oxide, TiO_2 can lower the pH value around MgH_2, which can therefore enhance the hydrolysis properties of MgH_2; $MgAl_2O_4$ has a catalytic effect on the hydrolysis of MgH_2; Fe as the cathode of galvanic cell and thereby reduce the activation energy for hydrolysis reaction of MgH_2. Awad et al. [26] studied the effect of adding carbon materials, metals (Ni, Fe, and Al), and metal oxides (Nb_2O_5 and V_2O_5) by using the ball grinding method on the hydrolysis of magnesium-based materials; it was found that the mixture of Mg–5 wt.% C–5 wt.% Ni had the best hydrolysis rate (95% of the theoretical hydrogen production within 2 minutes) and the lowest hydrolysis activation energy (14.34 kJ mol^{-1}). It was proven that the carbon material and the transition metal Ni could promote the hydrolysis of magnesium-based materials. However, the synergistic effect of carbon and metal oxides on magnesium has not been systematically studied, while the mechanism has not been analyzed [25, 26, 28].

Considering the above, in this paper, several MgH_2–C and MgH_2–C–Fe_2O_3 materials were prepared by hydrogenation after magnetic grinding. The synergistic effect of graphite and Fe_2O_3 on the hydrolytic kinetics of magnesium-based hydrogen storage materials was investigated systematically. The hydrolytic conversion rate, hydrolytic reaction rate, and hydrolytic activation energy Ea of pure MgH_2 and composite powders with different additives were obtained.

2. Experimental

2.1. Sample Preparation. Magnesium-based hydride composite materials were prepared by hydrogenation after magnetic grinding. The starting materials are Mg powder (purity ≥ 99%, 200 mesh, Sinopharm Chemical Reagent Co., Ltd), MgH_2, (purity ≥ 99.5%, MG Power Technology Co., Ltd), Fe_2O_3 (average particle size 20 nm, purity ≥ 99.5 %, Shanghai Yaoyi), and graphite (average particle size 80 nm, purity ≥ 99.5%, Shanghai Yaoyi). Place the required raw materials (total weight 3 g, MgH_2–C (Mg : C mass ratio = 0.95 : 0.05), MgH_2–C–Fe_2O_3 (Mg : C : Fe_2O_3 mass ratio = 0.9 : 0.05 : 0.05) into the stainless steel reaction kettle (volume 100 mL, 60 g of steel needle for grinding is installed in the reaction kettle, 0.3 × 5 mm : 1 × 5 mm mass ratio = 1 : 1). In order to prevent Mg oxidation during grinding, high purity Ar gas (99.999%) was used to purge the reactor chamber and pipeline for 20 min before grinding, and a small amount of Ar gas was filled in the chamber and pipeline for protection. Then, the grinding experiment was performed (rotational speed = 2400 rad/min), and the grinding time was 2 h (grinding 30 min + cooling 30 min, repeated four times). Then, the reactor was placed on a constant temperature heating furnace (~ 300°C) and filled with hydrogen gas (~ 2.3 MPa) for 2 h hydrogenation. Then, the furnace was cooling under room temperature and stood for 12 h. The samples were taken out after the reaction kettle which naturally cooled to room temperature. The powder composite of MgH_2–5 wt.% C and MgH_2–5 wt.% Fe_2O_3–5 wt.% C was prepared. The pure MgH_2 powder is also annealed in hydrogen gas.

2.2. Hydrolysis Experiment. The hydrolysis device is shown in Figure 1, which mainly consists of a reaction device and a collection device. The reaction device includes a thermostatic water bath pot, three-necked flask, and condensing tube. The flask's three mouths are, respectively, used for inserting a thermometer, connecting the condensing tube, and adding powder samples. The collecting device consists of a Monteggia washing bottle, beaker, and electronic balance. Adding 100 mL of municipal drinking water into a three-necked flask and using a water bath to control temperature. Then, adding 0.05 g powder into the three-necked flask and recording the time. Through the condenser tube, the condensed hydrogen enters the Monteggia washing bottle. The hydrogen drains the water from the Monteggia washing bottle to the beaker. The hydrogen released is estimated through calculating the weight of the discharged water.

The hydrogen conversion rate is the ratio of the amount of hydrogen produced at time T to the total amount of hydrogen produced by adding excess of 0.1 mol L^{-1} HCl solution [29] (see Table 1).

2.3. Sample Characterization. Components and crystal structures of the samples were examined by powder X–ray diffraction apparatus (XRD, Ultima IV, Rigaku Corporation) equipped with a Cu Kα radiation source. XRD analyses were performed over a range from 10° to 80° at a scanning rate of 10° min^{-1}. Using a scanning electron microscope (SEM, Quanta 250, FEI, equipped with energy dispersive spectroscopy (EDS) system, working voltage 20 kV) to observe the structure and element composition of the composite powder.

3. Results and Discussion

3.1. Composition and Structure of Mg Hydrogen Storage Materials Prepared. XRD patterns of the MgH_2–C and MgH_2–C–Fe_2O_3 powders are shown in Figures 2(a) and 2(b). It can be seen from Figure 2 that the MgH_2–C–Fe_2O_3 powder has diffraction peaks of MgH_2, Mg, MgO, and C, as well as a small diffraction peak of Fe_2O_3. And the MgH_2–C powder only showed diffraction peaks of MgH_2, Mg, MgO, and C. With the exception of MgH_2, neither of the two powders produced any new substances, which proved that no other side reactions during the magnetic grinding and hydrogenation. The appearance of the Mg diffraction peak is due to the fact that part of the Mg particles not sufficiently ground or agglomerated during the magnetic grinding process, resulting in the large particles of Mg not being completely hydrogenated. And the one reason for appearing MgO is that there is an oxide layer on the surface of the raw material Mg particles. The steel needle in the grinding chamber uses mechanical force

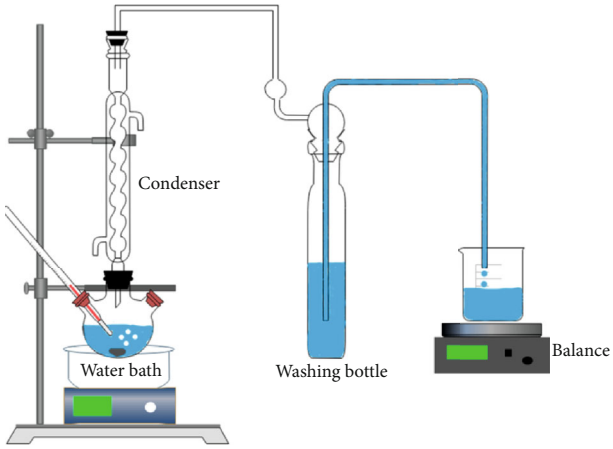

Figure 1: The experimental apparatus used for hydrolyzing hydrogen production.

Table 1: The amount of hydrogen released from each sample after complete hydrolysis.

Samples	Total hydrogen released [mL/g]
Pure MgH_2	1730
MgH_2–C	1602
MgH_2–C–Fe_2O_3	1503

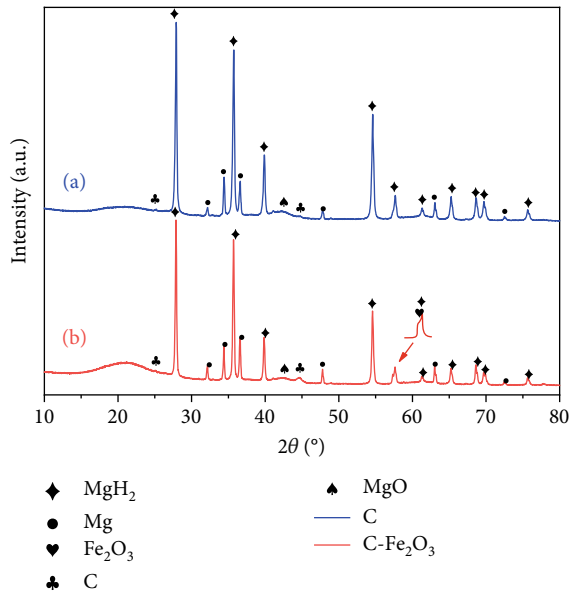

Figure 2: XRD patterns of MgH_2–C (a) and MgH_2–C–Fe_2O_3 (b) powders prepared by magnetic grinding and hydrogenation.

to cut the Mg particles while peeling off the surface MgO layer. MgO is mixed in the hydrogenated MgH_2 powder. Another reason for appearing MgO is the part of Mg that has not been completely hydrogenated quickly producing a dense MgO layer on the surface when it comes in contact with air. In addition, we also found that the diffraction peak strength of C and Fe_2O_3 is relatively low, which may be caused by the low content of these two phases, the excessively small particle size, and the relatively high dispersion.

The SEM measurements were taken out to characterize the structure of the MgH_2–C (Figure 3) and MgH_2–C–Fe_2O_3 (Figure 4). In Figures 3(c) and 3(d) and 4(c) and 4(d), it can be seen that the particle size of MgH_2 is relatively uniform, and the particle size of the two samples is about 300-700 nm. This is because the fine graphite particles are distributed on the surface and gap of the Mg during the magnetic grinding process to play a role of lubrication and dispersion, which reduces the cold welding phenomenon of Mg particles. This effectively prevents the agglomeration of Mg particles, so that the size of the hydrogenated MgH_2 particles is smaller and uniform, which is similar to the research conclusion of the ball milling reaction of C and Mg reported by Awad et al. [26]. Compared with the MgH_2–C powder (Figure 3(c)), the MgH_2–C–Fe_2O_3 powder (Figure 4(c)) has fewer large particles and a more even particle size, which indicates that the addition of Fe_2O_3 can further reduce the size of MgH_2 particles.

The SEM image and EDS spectrum of the MgH_2–C–Fe_2O_3 powder (Figure 4(b)) show that there is a certain amount of Fe on the surface of the particle. Combined with the XRD pattern of the sample (Figure 2(b)), it shows that the Fe element comes from Fe_2O_3, which further proves the presence of Fe_2O_3.

3.2. Kinetics of Hydrolysis. Figure 5 shows the hydrogen release curves of pure MgH_2 (a), MgH_2–C powder (b), and MgH_2–C–Fe_2O_3 powder (c) in municipal drinking water at 353 K. It can be observed that the hydrolysis rate of pure MgH_2 and the hydrogen conversion rate are relatively low. At 353 K, pure MgH_2 produces only 113 mL g^{-1} hydrogen in 2 minutes, 201.9 mL g^{-1} hydrogen in 5 minutes, and the hydrolysis conversion rate in 60 minutes is only 19.3%. It is possible that after the first few minutes of rapid reaction, a dense $Mg(OH)_2$ layer was formed on the surface of MgH_2, which prevented MgH_2 from further reacting with water. In contrast, when the C added sample is at 353 K, the hydrogen production is 268.5 mL g^{-1} in 2 minutes, 416 mL g^{-1} hydrogen is produced in 5 minutes, and the hydrolysis conversion rate is 52.5% in 60 minutes. The sample with C and Fe_2O_3 showed the fastest hydrolysis rate at 353 K, with 280 mL g^{-1} hydrogen produced in 2 minutes, 468 mL g^{-1} hydrogen produced in 5 minutes, and the hydrolysis conversion rate increased to 62.8% in 60 minutes. Compared with pure MgH_2, the two have better hydrolysis kinetics and higher hydrolysis conversion rate, which proves that C and Fe_2O_3 can promote the hydrolysis of MgH_2. This is because, in the magnetic grinding process, C can effectively reduce the agglomeration of magnesium particles, make the particle size of the hydrogenated powder smaller, increase the area in contact with water during hydrolysis, and thus effectively improve the hydrolysis reaction rate. Tayeh et al. [16] also showed a similar effect after ball milling of MgH_2 with C added. Fe_2O_3 can further reduce the particle size of MgH_2 and may have a catalytic effect on the hydrolysis reaction of MgH_2. Furthermore, it can improve the hydrolysis kinetic performance of MgH_2.

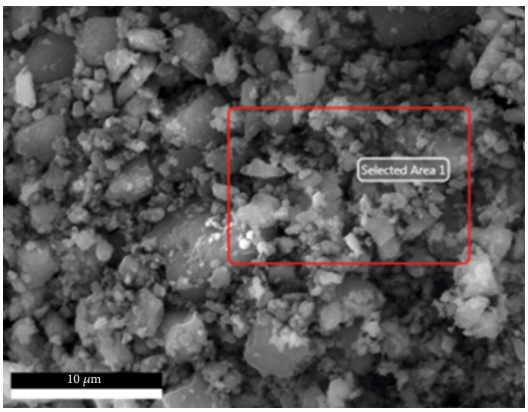

(a)

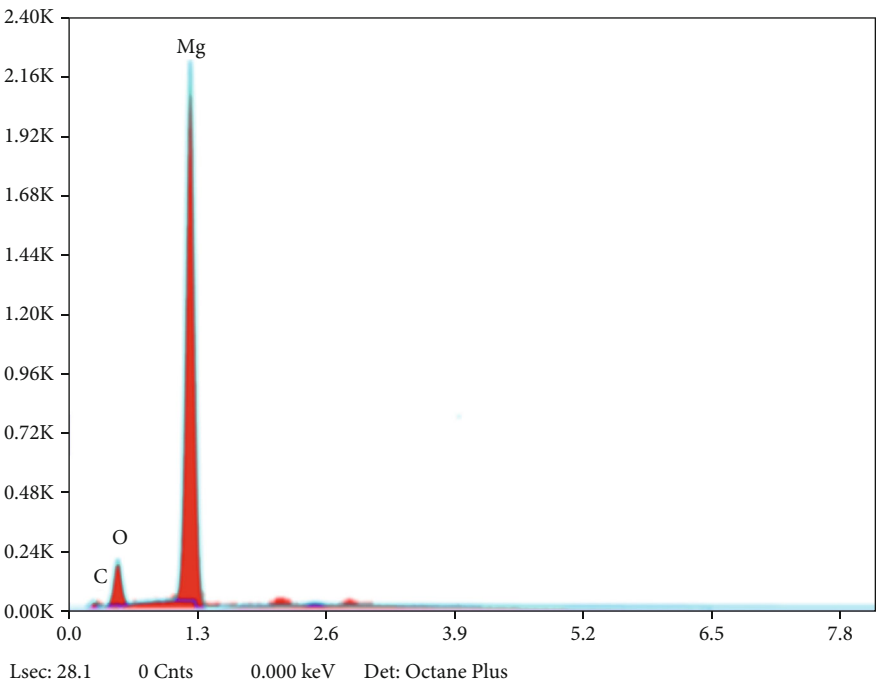

(b)

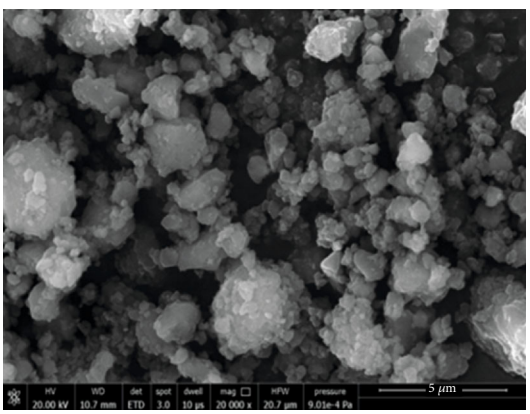

(c)

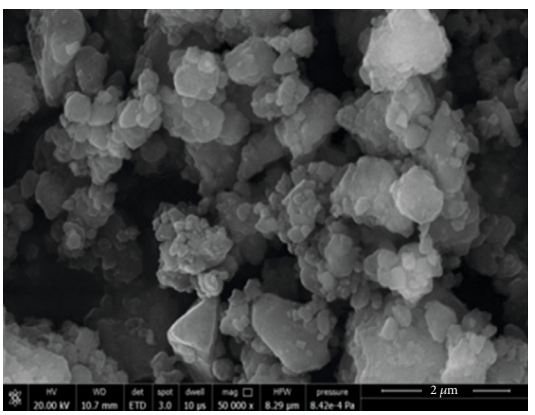

(d)

Figure 3: SEM micrograph of the MgH_2–C (a, c, d) and EDS analysis of (a).

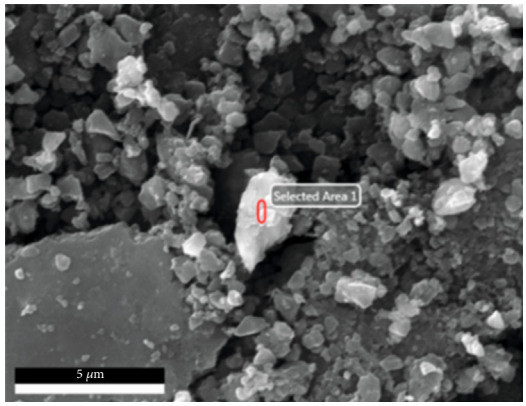

(a)

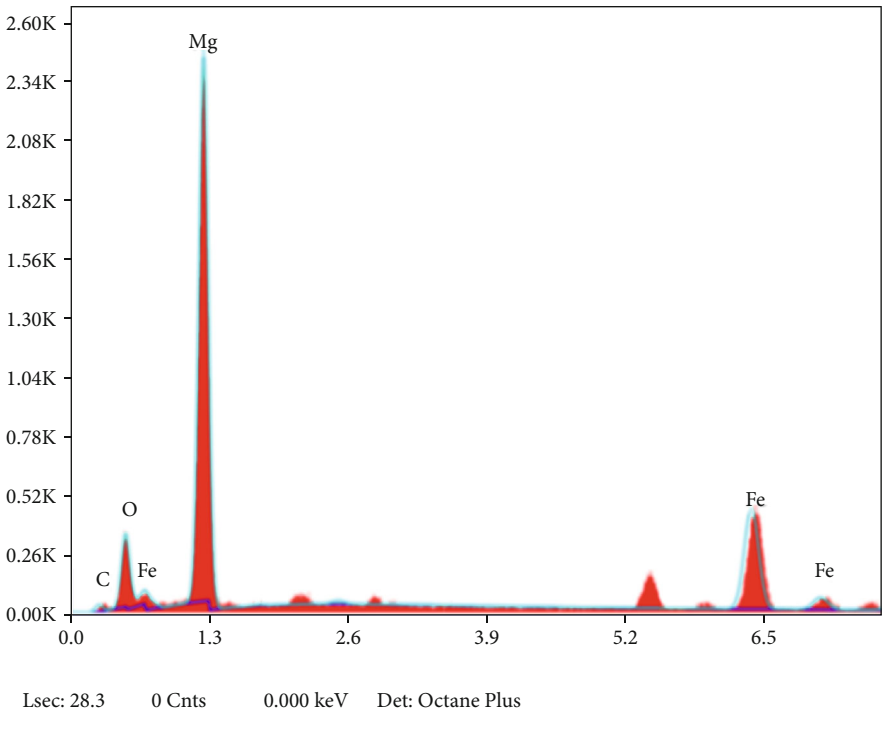

(b)

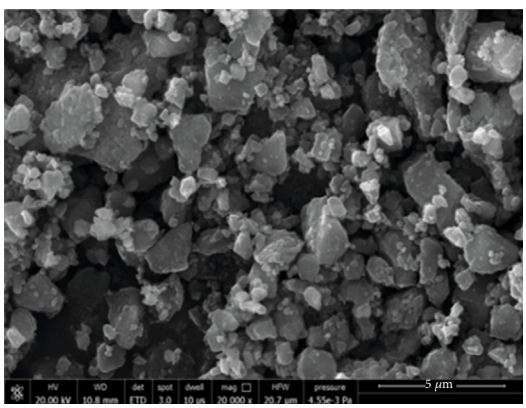

(c)

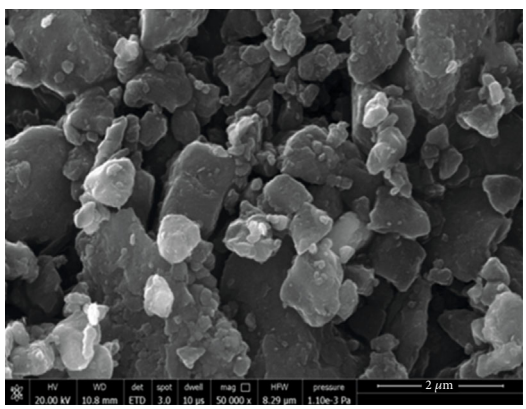

(d)

Figure 4: SEM micrograph of the MgH_2–C–Fe_2O_3 (a, c, d) and EDS analysis of (a).

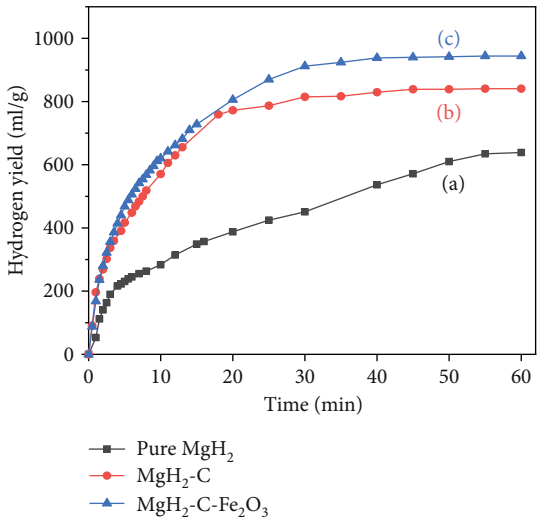

Figure 5: The hydrogen evolution curves for the hydrolysis of pure MgH_2 (a), MgH_2–C (b), and MgH_2–C–Fe_2O_3 (c) at 353 K.

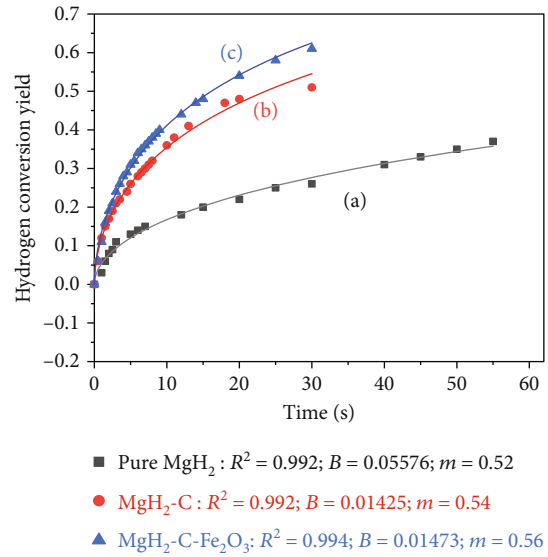

Figure 6: The kinetic curves of hydrogen generation for the hydrolysis of (a) pure MgH_2, (b) MgH_2–C, and (c) MgH_2–C–Fe_2O_3 at 353 K in municipal drinking water.

In order to investigate the synergistic effect of the addition of C and Fe_2O_3 on the hydrolytic hydrogen production performance of MgH_2, we tested the hydrogen liberation performance of pure MgH_2, MgH_2–C powder, and MgH_2–C–Fe_2O_3 powder in municipal drinking water under different temperature conditions. As shown in Figure S1, compared with pure MgH_2 and MgH_2–C powders, the hydrogen production rate and hydrogen conversion rate of MgH_2–C–Fe_2O_3 powder are greatly improved at different temperatures. Figure S1(c) shows that MgH_2–C–Fe_2O_3 powder has the highest hydrogen production rate and hydrogen conversion rate. Compared with MgH_2–C powder, the hydrogen conversion rate increases from 28.6% to 36.4% at 333 K (see Table S1) and from 50.9% to 60.7% in the first 30 min at 353 K (see Table S2), respectively. The results show that the synergistic effect of C and Fe_2O_3 together can significantly improve the hydrolysis kinetics of MgH_2 and increase the hydrogen conversion rate.

Two main models, the diffusion-controlled and the phase-boundary controlled, describe the experimental kinetic curves of MgH_2 hydrolysis [30]. The hydrolysis process of MgH_2 and MgH_2–additives in municipal drinking water can be described by the Avramie–Erofeev equation (Equation (2)) [20]:

$$\alpha(t) = 1 - \exp\left(-Bt^m\right). \quad (2)$$

$\alpha(t)$ is the reaction rate (the ratio of the amount of reacted material to the total amount of material, it can be regarded as hydrogen conversion rate), t is the reaction time, and B and m are constants. Values of B and m obtained by fitting and R^2 (correlation coefficient) are shown in Figure 6. The R^2 values indicate that the fitted results are in good agreement with the experimental data. Different m values represent different nucleation growth rate control steps, and m values for one-dimensional diffusion and for three-dimensional interfacial reaction are 0.62 and 1.07, respectively [20]. According to Figure 6, the m values of MgH_2–C–Fe_2O_3, MgH_2–C, and pure MgH_2 samples are 0.56, 0.54, and 0.52, respectively, which are closer to 0.62. This indicates that the hydrolysis of three samples at 353 K follows a one-dimensional diffusion mechanism.

3.3. Activation Energy of Hydrolysis. The apparent activation energy for hydrolysis of MgH_2 can be determined by the Arrhenius equation (Equation (3)):

$$k = A \cdot \exp\left(-\mathrm{Ea}/RT\right), \quad (3)$$

where k is the reaction rate constant, Ea is the apparent activation energy ($J\,mol^{-1}$), R is the molar gas constant ($8.314\,J\,mol^{-1}\,K^{-1}$), and T is the reaction temperature (K). By fitting the lnk–1000/T line, the slope of the line was multiplied by the R value, and the apparent activation energy Ea of different samples was finally obtained. Figure 7 shows the apparent activation energy of three different samples calculated. R^2 values in all cases are >0.98, indicating that the Arrhenius equation is appropriate for describing the hydrolysis of MgH_2. From the slope of the fitted line, Ea of pure MgH_2 was found to be $55.57\,kJ\,mol^{-1}$. Similarly, Ea values of MgH_2–C and MgH_2–C–Fe_2O_3 samples were 43.40 and $36.92\,kJ\,mol^{-1}$, respectively, which were lower than the value for pure MgH_2. It can be seen that adding C can reduce the hydrolysis activation energy of MgH_2; adding C and Fe_2O_3 at the same time can further reduce the hydrolysis activation energy of MgH_2. A lower Ea value generally indicates a higher reaction activity. Therefore, the addition of C and Fe_2O_3 simultaneously has a synergistic effect on improving the hydrolysis properties of MgH_2.

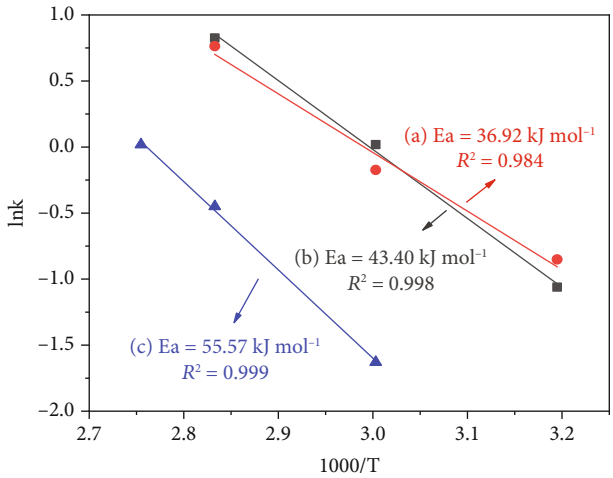

Figure 7: Arrhenius plot for the activation energy calculation hydrolysis of MgH_2–C–Fe_2O_3 (a), MgH_2–C (b), and pure MgH_2 (c) in municipal drinking water.

4. Conclusion

In this work, MgH_2–C and MgH_2–C–Fe_2O_3 composite powders were prepared by the hydrogenation after magnetic grinding. The effects of graphite and Fe_2O_3 on the hydrolysis kinetics of MgH_2 were studied. It was found that both MgH_2–C and MgH_2–C–Fe_2O_3 samples have better performance of hydrolysis reaction rate and hydrogen conversion rate compared with pure MgH_2. Among them, MgH_2–C–Fe_2O_3 sample has the fastest hydrolytic yield rate and the highest conversion rate. The conversion rate of 30 minutes at 353 K is 9.8% higher than that of the MgH_2–C sample, while that is 42.6% higher than that of pure MgH_2. It was also found that the Ea value of hydrolysis activation energy of pure MgH_2 was 55.57 kJ mol^{-1}. The addition of C and Fe_2O_3 could effectively reduce the Ea value of MgH_2–C and MgH_2–C–Fe_2O_3 samples to 43.40 and 36.92 kJ mol^{-1}, respectively. The results show that the addition of graphite and Fe_2O_3 has an obvious synergistic effect on improving the hydrolysis kinetics and hydrogen conversion rate of MgH_2.

Abbreviations

ΔH: Reaction enthalpy
$\alpha(t)$: Hydrogen conversion rate
B: Constant
t: Reaction time
m: Constant
k: Reaction rate constant
Ea: Hydrolysis activation energy
A: Preexponential factor
R: Molar gas constant
T: Reaction temperature.

Data Availability

All data used to support the this study are available from the corresponding author upon request.

Conflicts of Interest

The authors declare no conflict of interest.

Authors' Contributions

Kun Yang and Hongyun Qin contributed equally to this work.

Acknowledgments

This work is financially supported by the National Natural Science Foundation of China (No. 51976112).

Supplementary Materials

Figure S1: the hydrogen evolution curves for the hydrolysis of (a) pure MgH_2, (b) MgH_2–C, and (c) MgH_2–C–Fe_2O_3 in municipal drinking water at different temperatures. Table S1: hydrogen conversion rate at 333 K. Table S2: hydrogen conversion rate at 353 K. *(Supplementary Materials)*

References

[1] Q. Lai, M. Paskevicius, D. A. Sheppard et al., "Hydrogen storage materials for mobile and stationary applications: current state of the art," *Chensuschem*, vol. 8, no. 17, pp. 2789–2825, 2015.

[2] M. Rueda, L. M. Sanz-Moral, and Á. Martín, "Innovative methods to enhance the properties of solid hydrogen storage materials based on hydrides through nanoconfifinement: a review," *The Journal of Supercritical Fluids*, vol. 141, pp. 196–217, 2018.

[3] L. Ouyang, M. Ma, M. Huang et al., "Enhanced hydrogen generation properties of MgH_2-based hydrides by breaking the magnesium hydroxide passivation layer," *Energies*, vol. 8, no. 5, pp. 4237–4252, 2015.

[4] M. Huang, L. Ouyang, Z. Chen, C. Peng, X. Zhu, and M. Zhu, "Hydrogen production via hydrolysis of Mg-oxide composites," *International Journal of Hydrogen Energy*, vol. 42, no. 35, pp. 22305–22311, 2017.

[5] M. Ni, M. K. H. Leung, D. Y. C. Leung, and K. Sumathy, "A review and recent developments in photocatalytic water-splitting using TiO_2 for hydrogen production," *Renewable & Sustainable Energy Reviews*, vol. 11, no. 3, pp. 401–425, 2007.

[6] L. Ouyang, J. Huang, H. Wang et al., "Excellent hydrolysis performances of Mg_3RE hydrides," *International Journal of Hydrogen Energy*, vol. 38, no. 7, pp. 2973–2978, 2013.

[7] L. Ouyang, Y. Xu, H. Dong, L. X. Sun, and M. Zhu, "Production of hydrogen via hydrolysis of hydrides in Mg-La system," *International Journal of Hydrogen Energy*, vol. 34, no. 24, pp. 9671–9676, 2009.

[8] L. Ouyang, H. Zhong, Z. Li et al., "Low-cost method for sodium borohydride regeneration and the energy efficiency of its hydrolysis and regeneration process," *Journal of Power Sources*, vol. 269, pp. 768–772, 2014.

[9] M. Fan, F. Xu, and L. Sun, "Studies on hydrogen generation characteristics of hydrolysis of the ball milling Al-based materials in pure water," *International Journal of Hydrogen Energy*, vol. 32, no. 14, pp. 2809–2815, 2007.

[10] C. Haertling, R. J. Hanrahan, and R. Smith, "A literature review of reactions and kinetics of lithium hydride hydrolysis," *Journal of Nuclear Materials*, vol. 349, no. 1-2, pp. 195–233, 2006.

[11] C. Ward, D. Stanga, L. Pataki, and R. D. Venter, "Design for the cold start-up of a man-portable fuel cell and hydrogen storage system," *Journal of Power Sources*, vol. 41, no. 3, pp. 335–352, 1993.

[12] W. Chen, L. Ouyang, J. Liu et al., "Hydrolysis and regeneration of sodium borohydride ($NaBH_4$) - A combination of hydrogen production and storage," *Journal of Power Sources*, vol. 359, pp. 400–407, 2017.

[13] Z. Xiong, L. Cao, J. Wang, and J. Mao, "Hydrolysis behavior of $LiBH_4$ films," *Journal of Alloys and Compounds*, vol. 698, pp. 495–500, 2017.

[14] Y. Zhu, L. Ouyang, H. Zhong et al., "Closing the loop for hydrogen storage: facile regeneration of NaBH4from its hydrolytic product," *Angewandte Chemie, International Edition*, vol. 59, no. 22, pp. 8623–8629, 2020.

[15] Y. Kojima, K. I. Suzuki, and Y. Kawai, "Hydrogen generation by hydrolysis reaction of magnesium hydride," *Journal of Materials Science*, vol. 39, no. 6, pp. 2227–2229, 2004.

[16] T. Tayeh, A. S. Awad, M. Nakhl, M. Zakhour, J. F. Silvain, and J. L. Bobet, "Production of hydrogen from magnesium hydrides hydrolysis," *International Journal of Hydrogen Energy*, vol. 39, no. 7, pp. 3109–3117, 2014.

[17] J. Huot, G. Liang, and R. Schulz, "Magnesium-based nanocomposites chemical hydrides," *Journal of Alloys and Compounds*, vol. 353, no. 1–2, pp. L12–L15, 2003.

[18] Ç. Öz, B. Coşkuner Filiz, and A. Kantürk Figen, "The effect of vinegar-acetic acid solution on the hydrogen generation performance of mechanochemically modified magnesium (Mg) granules," *Energy*, vol. 127, pp. 328–334, 2017.

[19] J. Chen, H. Fu, Y. Xiong, J. Xu, J. Zheng, and X. Li, "$MgCl_2$ promoted hydrolysis of MgH_2 nanoparticles for highly efficient H_2 generation," *Nano Energy*, vol. 10, pp. 337–343, 2014.

[20] M. Huang, L. Ouyang, H. Wang, J. Liu, and M. Zhu, "Hydrogen generation by hydrolysis of MgH_2 and enhanced kinetics performance of ammonium chloride introducing," *International Journal of Hydrogen Energy*, vol. 40, no. 18, pp. 6145–6150, 2015.

[21] D. Gan, Y. Liu, J. Zhang et al., "Kinetic performance of hydrogen generation enhanced by $AlCl_3$ via hydrolysis of MgH_2 prepared by hydriding combustion synthesis," *International Journal of Hydrogen Energy*, vol. 43, no. 22, pp. 10232–10239, 2018.

[22] S. Wang, L. Sun, F. Xu et al., "Hydrolysis reaction of ball-milled Mg-metal chlorides composite for hydrogen generation for fuel cells," *International Journal of Hydrogen Energy*, vol. 37, no. 8, pp. 6771–6775, 2012.

[23] H. Wang, J. Zhang, J. Liu, L. Z. Ouyang, and M. Zhu, "Catalysis and hydrolysis properties of perovskite hydride $NaMgH_3$," *Journal of Alloys and Compounds*, vol. 580, pp. S197–S201, 2013.

[24] J. P. Tessier, P. Palau, J. Huot, R. Schulz, and D. Guay, "Hydrogen production and crystal structure of ball-milled MgH_2-Ca and MgH_2-CaH_2 mixtures," *Journal of Alloys and Compounds*, vol. 376, no. 1-2, pp. 180–185, 2004.

[25] M. Ma, L. Yang, L. Ouyang, H. Shao, and M. Zhu, "Promoting hydrogen generation from the hydrolysis of Mg-graphite composites by plasma-assisted milling," *Energy*, vol. 167, pp. 1205–1211, 2019.

[26] A. S. Awad, E. El-Asmar, T. Tayeh et al., "Effect of carbons (G and CFs), TM (Ni, Fe and Al) and oxides (Nb_2O_5 and V_2O_5) on hydrogen generation from ball milled Mg-based hydrolysis reaction for fuel cell," *Energy*, vol. 95, pp. 175–186, 2016.

[27] S. Hong, H. Kim, and M. Y. Song, "Rate enhancement of hydrogen generation through the reaction of magnesium hydride with water by MgO addition and ball milling," *Journal of Industrial and Engineering Chemistry*, vol. 18, no. 1, pp. 405–408, 2012.

[28] B. Yang, J. Zou, T. Huang, J. Mao, X. Zeng, and W. Ding, "Enhanced hydrogenation and hydrolysis properties of core-shell structured Mg–MOx (M = Al, Ti and Fe) nanocomposites prepared by arc plasma method," *Chemical Engineering Journal*, vol. 371, pp. 233–243, 2019.

[29] R. V. Lukashev, N. A. Yakovleva, S. N. Klyamkin, and B. P. Tarasov, "Effect of mechanical activation on the reaction of magnesium hydride with water," *Russian Journal of Inorganic Chemistry*, vol. 53, no. 3, pp. 389–396, 2008.

[30] N. Senes, L. Fernández Albanesi, S. Garroni et al., "Kinetics and hydrogen storage performance of Li-Mg-N-H systems doped with Al and $AlCl_3$," *Journal of Alloys and Compounds*, vol. 765, pp. 635–643, 2018.